Isenman, D. E., Dorrington, K. J., & Painter, R. H. (1975) *J. Immunol. 114*, 1726–1729.
Kabat, E. A., Wu, T. T., & Bilofsky, H. (1979) NIH Publication No. 80-2008, Bethesda, MD.
Kawato, S., Kinosita, K., Jr., & Ikegami, A. (1978) *Biochemistry 17*, 5026–5031.
Luedtke, R., Owen, C. S., & Karush, F. (1980) *Biochemistry 19*, 1182–1192.
Means, G. E., & Feeney, R. E. (1971) in *Chemical Modification of Proteins*, Chapter 6, pp 105–110, Holden-Day, San Francisco, CA.
Metzger, H. (1974) *Adv. Immunol. 18*, 169–207.
Metzger, H. (1978) *Contemp. Top. Mol. Immunol. 7*, 119–152.
Michaelsen, Y. E., Wisloff, F., & Natvig, J. B. (1975) *Scand. J. Immunol. 4*, 71–78.
Parker, C. W., Yoo, T. J., Johnson, M. C., & Godt, S. M. (1967) *Biochemistry 6*, 3408–3416.
Poljak, R. J. (1975) *Nature (London) 256*, 373–376.
Rockey, J. H., Montgomery, P. C., Underdown, B. J., & Dorrington, K. J. (1972) *Biochemistry 11*, 3172–3181.
Romans, D. G., Tilley, C. A., Crokkston, M. C., Falk, R. E., & Dorrington, K. J. (1977) *Proc. Natl. Acad. Sci. U.S.A. 74*, 2531–2535.
Sakano, H., Rogers, J. H., Hüppi, K., Brock, C., Traunecher, A., Maki, R., Wall, R., & Tonegawa, S. (1979) *Nature (London) 277*, 627–633.
Schlessinger, J., Steinberg, I. Z., Givol, D., Hochman, J., & Pecht, I. (1975) *Proc. Natl. Acad. Sci. U.S.A. 72*, 2775–2779.
Stevenson, G. T., & Dorrington, K. J. (1970) *Biochem. J. 118*, 703–712.
Stryer, L. (1978) *Annu. Rev. Biochem. 47*, 819–846.
Vanderkooi, J., Erecińska, M., & Chance, B. (1973) *Arch. Biochem. Biophys. 154*, 219–229.
Van Der Meulen, J. A., McNabb, T. C., Haeffner-Cavaillon, N., Klein, M., & Dorrington, K. J. (1980) *J. Immunol. 124*, 500–507.
Venyaminov, S. Y., Rajnavölgyi, E., Medgyesi, G. A., Gergely, J., & Zavodsky, P. (1976) *Eur. J. Biochem. 67*, 81–86.
Vuk-Pavlović, S., Blatt, Y., Glaudemans, C. P. J., Lancet, D., & Pecht, I. (1978) *Biophys. J. 24*, 161–174.
Wahl, P. (1975) *Biochem. Fluoresc. Concepts 1*, 1–41.
Wu, C., & Stryer, L. (1972) *Proc. Natl. Acad. Sci. U.S.A. 69*, 1104–1108.
Yasmeen, D., Ellerson, J. R., Dorrington, K. J., & Painter, R. H. (1976) *J. Immunol. 116*, 518–527.
Yguerabide, J. (1972) *Methods Enzymol. 26*, 498–577.

Role of Tryptophanyl and Tyrosyl Residues of Flavoproteins in Binding with Flavin Coenzymes. X-ray Structural Studies Using Model Complexes†

Masatoshi Inoue, Megumi Shibata, Yu-ichi Kondo, and Toshimasa Ishida*

ABSTRACT: The crystal structures of 7,8-dimethylisoalloxazine-10-acetic acid–tryptamine (1:1) tetrahydrate and 7,8-dimethylisoalloxazine-10-acetic acid–tyramine (1:1) tetrahydrate complexes were determined by the X-ray diffraction method, as models for flavin–tryptophan and flavin–tyrosine interactions in flavoproteins. The observed parallel stackings and the intermolecular spacing distances, which were less than the normal van der Waals separation between the isoalloxazine and indole rings and between the isoalloxazine and phenol rings, suggest the existence of charge-transfer interactions in their ground states. The indole and phenol rings interact with the pyrimidinoid and pyrazinoid portions of the isoalloxazine ring and have short contacts, <3.4 Å, with the reduction site (N1 and N5 atoms) of this ring. This suggests that the reduction of oxidized flavin to the semiquinone state may be facilitated by charge transfer from the former rings to the N1 and N5 atoms. Absorption difference spectra showed that both complexes associate with equimolar ratios in solution as well as in the crystalline state and that they have the same charge-transfer bands and association constants as flavin mononucleotide (FMN)–Trp and FMN–Tyr complexes, respectively. On the other hand, proton magnetic resonance spectra suggested that in solution, the stacking modes of the indole and phenol rings to the isoalloxazine ring are different from those observed in the crystal structures and both aromatic rings are stacked over the whole of the isoalloxazine ring.

In living cells, flavoprotein require flavins such as FMN[1] and FAD for effective oxidation–reduction catalyses. For an understanding of the mechanism of action of flavoproteins, which are formed via a simple biomolecular process, i.e., apoprotein + flavin ⇌ flavoprotein, the details of the flavin–apoprotein interaction need to be elucidated. Information gained by diverse spectral studies of native and chemically modified flavoproteins, augmented by X-ray crystallography, provides unequivocal evidence for the interaction of the flavin isoalloxazine ring with aromatic amino residues within the flavin-binding sites of numerous flavoproteins [for reviews, see Mayhew & Ludwig (1975) and McCormick (1977)]. For instance, X-ray studies on flavodoxin from *Desulfovibrio vulgaris* (Watenpaugh et al., 1973) showed that Trp-60 and Tyr-99 residues are involved in cofactor binding with FMN. Table I lists the some flavoproteins in which the aromatic amino acid participates in the binding with flavin; obviously,

† From the Department of Physical Chemistry, Osaka College of Pharmacy, 2-10-65 Kawai, Matsubara-City, Osaka 580, Japan. *Received October 24, 1980.* This work is part VII of "Structural Studies of the Interaction between Indole Derivatives and Biologically Important Aromatic Compounds". Reference Ishida et al. (1980) is an earlier study in this series.

[1] Abbreviations used: DIA, 7,8-dimethylisoalloxazine-10-acetic acid; TPA, tryptamine; TRA, tyramine; DSS, 2,2-dimethyl-2-silapentane-5-sulfonate; PMR, proton magnetic resonance; CNDO/2, complete neglect of differential overlap; FMN, flavin mononucleotide; FAD, flavin adenine dinucleotide.

0006-2960/81/0420-2936$01.25/0

Table I: List of Aromatic Amino Acids Necessary for Binding with Flavin in Flavoprotein

enzyme	source	flavin	amino acid	method	reference
flavodoxin	*Clostridium MP*	FMN	Trp	X-ray[a]	Burnett et al., 1974
	Desulfovibrio vulgaris	FMN	Tyr, Trp	X-ray	Watenpaugh et al., 1973
	Clostridium pasteurignum	FMN	Trp	spectra[b]	McCormick, 1970
	Azotobacter vinelandii	FMN	Trp	spectra	Andrews et al., 1973
		FMN	Trp	spectra	Ryan & Tollin, 1973
flavocytochrome c_{552}	*Chromatium*	FAD	Tyr	spectra	Kenney et al., 1974
cytochrome b_5 reductase	calf liver	FAD	Tyr	spectra	Strittmatter, 1961
D-amino-acid oxidase	hog kidney	FAD	Tyr	spectra	Tu & McCormick, 1973
		FAD	Trp	spectra	Wu et al., 1970
old yellow enzyme	yeast	FMN	Tyr	spectra	Nygaard & Theorell, 1955
egg white flavoprotein	hen	riboflavin	Tyr, Trp	spectra	Blankenhorn, 1978
	hen	riboflavin	Tyr, Trp	spectra	Nishikimi & Kyogoku, 1973
egg yolk flavoprotein	hen	riboflavin	Trp	spectra	Steczko & Ostrowski, 1975

[a] X-ray crystallographic method. [b] Various spectroscopic methods using native and chemically modified flavoproteins.

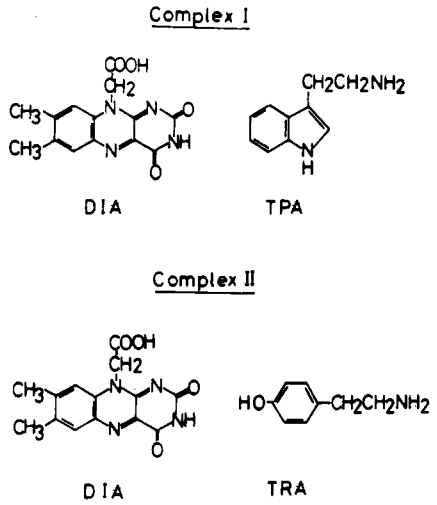

FIGURE 1: Model complexes used for studies on tryptophan–flavin and tyrosine–flavin interactions.

tryptophanyl and/or tyrosyl residues are essential for this binding. Spectral studies in solution, using model systems [McCormick, 1977; Slifkin (1971) and references therein], suggested that, due to the charge-transfer interaction, tryptophan and tyrosine derivatives could form molecular complexes with flavin derivatives. Since the indole ring of tryptophan and the phenol ring of tyrosine are electron donors compared with the isoalloxazine ring of flavin (Pullman & Pullman, 1963), the charge-transfer forces could be responsible for the binding with flavin in flavoprotein.

Table I also shows that, in the oxidation–reduction reaction, the biological functions of the tryptophanyl residue could be substituted for those of the tyrosyl residue.

To elucidate the modes and similarities of the interactions in flavin–tryptophan and flavin–tyrosine complexes at the molecular level, we determined the crystal structures of their model complexes by the X-ray diffraction method. They are the first models for flavin–indole and flavin–phenol charge-transfer interactions to be investigated directly at the molecular level. As a model for flavin, DIA,[1] which behaves like FMN in flavin-sensitized photooxiddation of tryptophan and tyrosine (Wu & McCormick, 1971), was selected. TPA and TRA were the models for tryptophan and tyrosine, respectively (Figure 1).

The structures of complexes I and II have been described briefly (Inoue et al., 1980; Ishida et al., 1979a). We now report the details of crystallographic results on complexes I and II and the charge-transfer interactions and their features in crystalline state and in solution. Our findings may provide important information in the study of the interaction between flavin and apoprotein in flavoprotein.

Table II: Crystal Data

	complex I	complex II
chemical formula	$C_{14}H_{12}N_4O_4 \cdot C_{10}H_{12}N_2 \cdot 4H_2O$	$C_{14}H_{12}N_4O_4 \cdot C_8H_{11}NO \cdot 4H_2O$
molecular weight	532.55	509.52
crystal system	monoclinic	monoclinic
space group	$P2_1/c$	$P2_1/c$
cell constant		
a (A)	18.604 (11)	10.724 (3)
b (A)	7.019 (1)	11.647 (4)
c (A)	19.435 (12)	19.728 (11)
β (deg)	100.63 (8)	96.67 (3)
volume (A^3)	2495 (9)	2448 (2)
Z	4	4
D_m (g·cm^{-3})	1.383 (1)	1.357 (1)
D_x (g·cm^{-3})	1.418	1.383
μ(Cu Kα) (cm^{-1})	7.37	7.61

Experimental Procedures

Preparation and X-ray Data Collection. DIA was synthesized from riboflavin as described by Fall & Petering (1956) and Föry et al. (1968). The addition of an equimolar amount of TPA or TRA molecules to the aqueous suspension of DIA increased its solubility and produced a color change from yellow to dark red (complex I) or red (complex II), suggesting the formation of a charge-transfer complex. Letting the aqueous solutions stand at room temperature for 1–2 weeks resulted in unstable platelet crystals of complexes I (dark red) and II (red). UV spectra of these crystals dissolved in water and thermal analyses suggested that both crystals are constituted of an equimolar ratio of the respective components and contain four crystal waters per complex. A single crystal for complex I (0.4 × 0.2 × 0.05 mm) or complex II (0.4 × 0.1 × 0.05 mm), sealed in a glass capillary tube in the presence of some mother liquid, was used for X-ray studies.

Preliminary oscillation and Weissenberg photographs showed both crystals to be monoclinic and in space group $P2_1/c$ from systematic absences. The crystallographic data are given in Table II. The calculated densities, containing four formula units in a unit cell, are not in good agreement with experimental values obtained by the flotation method using a benzene–carbon tetrachloride mixture; this may be ascribable to the dissociation of crystal waters. The cell constants of both crystals were determined on a four-circle diffractometers (Rigaku Denki Co., Japan) and refined by the least-squares method. Three-dimensional intensity data were collected with the same diffractometer, using graphite–monochromated Cu Kα radiation. By means of the $\omega/2\theta$ scan technique, all intensities of 4273 (complex I) and 4285 (complex II) inde-

pendent reflections, within $\sin\theta/\lambda < 0.588$ Å^{-1}, were collected at a rate of 4 °C/min; the background was counted for 5 s at the edges of the reflections. As the intensity of four standard reflections, monitored at 50 reflection intervals, decreased proportionally to the radiation time, the intensities were corrected on the basis of these decreases. Lorentz and polarization corrections were applied, but absorption corrections were not made for either complex, because the smallness of the crystal was thought to obviate severe absorption problems.

Structure Determination and Refinement of Complex I. The structure was determined by a combination of direct and Patterson vector search methods. Initial attempts to determine the structure by the direct method (MULTAN) (Germain et al., 1971) were in combination with a wide variety of modifications to the E set and to the starting phase set. Many of the calculated E maps revealed the isoalloxazine ring, so that a correct phase set could not be determined unequivocally. On the other hand, a Patterson map clearly revealed the orientation of the isoalloxazine ring; it was almost parallel to the a–c plane. Calculation of the minimum function; using 14 peaks corresponding to the isoalloxazine ring, showed two further isoalloxazine rings in a unit cell; these were related by a center of symmetry and a c-glide plane. The translated coordinates corresponding to space group $P2_1/c$ were in good agreement with a set of coordinates calculated by the direct method, which had a rather lower figure of merit (1.09) than the others. The calculated coordinates of the isoalloxazine ring were used for the further determination of the crystal structure. Careful inspection of the Fourier map made it possible to locate the indole ring. After five cycles of successive Fourier syntheses, the positions of all the remaining nonhydrogen atoms were determined. The structure was then refined by the full-matrix least-squares method with isotropic thermal parameters and then by the block-diagonal least-squares method with anisotropic temperature factors ($R = 0.14$), where the weights (w) were taken as unity. At this stage, a difference Fourier map showed the positions of all hydrogen atoms, except those of waters. They were included in all subsequent refinements with isotropic temperature factors. The final least-squares refinements were computed with a weighting scheme as follows: $w = 1.0$ for $F_0 \leq 36.0$ and $w = 1.0/[1.0 + 0.125(F_0 - 36.0)]$ for $F_0 > 36.0$. In the last cycle of refinement, none of the positional parameters shifted more than one-fourth of the estimated standard deviations. The final R value was 0.079, excluding $F_0 = 0.0$. (See paragraph at end of paper regarding supplementary material.)

Structure Determination and Refinement of Complex II. The structure was solved by the direct method (MULTAN). An E map with the highest figure of merit revealed the positions of all nonhydrogen atoms. The structure was refined by procedures similar to those applied to complex I. All hydrogen atoms, except those of waters and a hydrogen atom of amino group, were found by a difference Fourier map at the stage of $R = 0.15$. The final least-squares refinements were computed with a weighting scheme as follows: $w = 1.0$ for $F_0 \leq 5.0$ and $w = 1.0/[1.0 + 0.176(F_0 - 5.0)]$ for $F_0 > 5.0$. In the last cycle of refinement, none of the positional parameters shifted more than one-fourth of the estimated standard deviations. The final R value was 0.11, excluding $F_0 = 0.0$. For all computations, the UNICS system program (Ashida, 1973) was used; the atomic scattering factors were those cited in *International Tables for X-Ray Crystallography* (Cromer & Waber, 1974).

Molecular Orbital Calculation. The calculations of respective DIA, TPA, and TRA molecules were carried out by using the coordinates obtained by X-ray analyses and the molecular orbital CNDO/2 method (Pople & Segal, 1966). The stability of the electronic energy was used as a check for convergence in the iteration calculation.

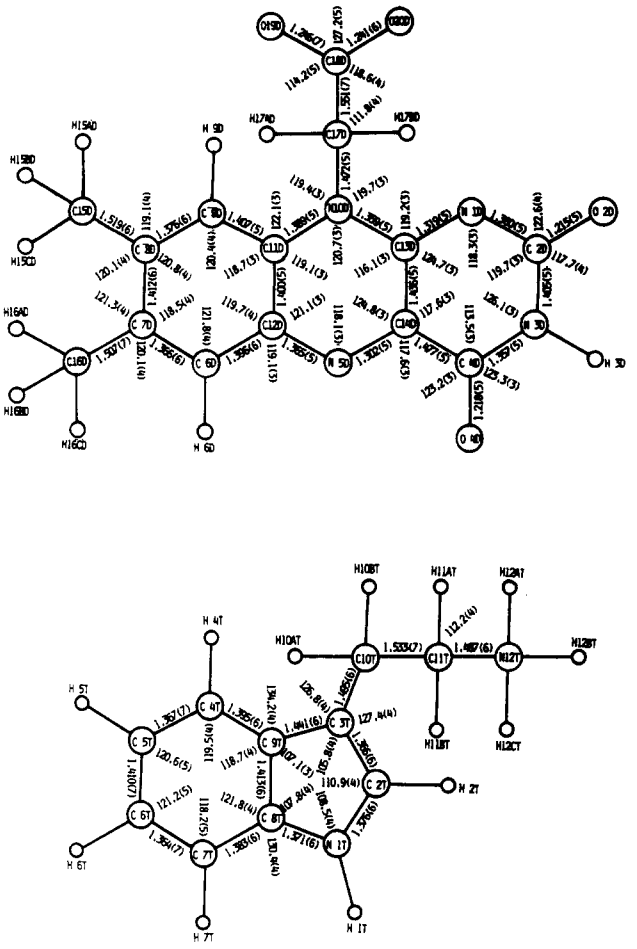

FIGURE 2: Complex I. Bond lengths (in angstroms) and angles (in degrees) between nonhydrogen atoms, along with the numbering used in this work.

Absorption Spectra. The electronic absorption spectra in the 300–650-nm range at 25 °C were recorded on a Hitachi 624 spectrophotometer with 10-mm cells. The spectra were measured 3 times in 0.025 M phosphate buffer containing 30% ethanol (pH 6.9) and averaged.

Proton Magnetic Resonance (PMR) Spectra. PMR spectra (90 MHz) of samples dissolved in 50% CD_3OD–D_2O solution were recorded in the continuous-wave mode (5-mm tubes) on a Hitachi Perkin-Elmer spectrometer at 31 °C. The values of chemical shifts were determined by reference to an internal standard (DSS).

All numerical calculations were carried out on an ACOS-700 computer of the Computation Center of Osaka University.

Results and Discussion

The coordinates of nonhydrogen atoms from the last refinement are given in Table III; the bond lengths and angles for nonhydrogen atoms with their standard deviations are given in Figures 2 (complex I) and 3 (complex II), together with the atomic numbering used in this work.

Molecular Structure of Complex I. The covalent bonding parameters of the isoalloxazine ring are in close agreement with the corresponding quantities of the "idealized" lumiflavin molecule (Wang & Fritchie, 1973). In the lengths, the average deviation from the idealized values is 0.005 Å. The isoalloxazine ring is approximately, but not strictly, planar with the

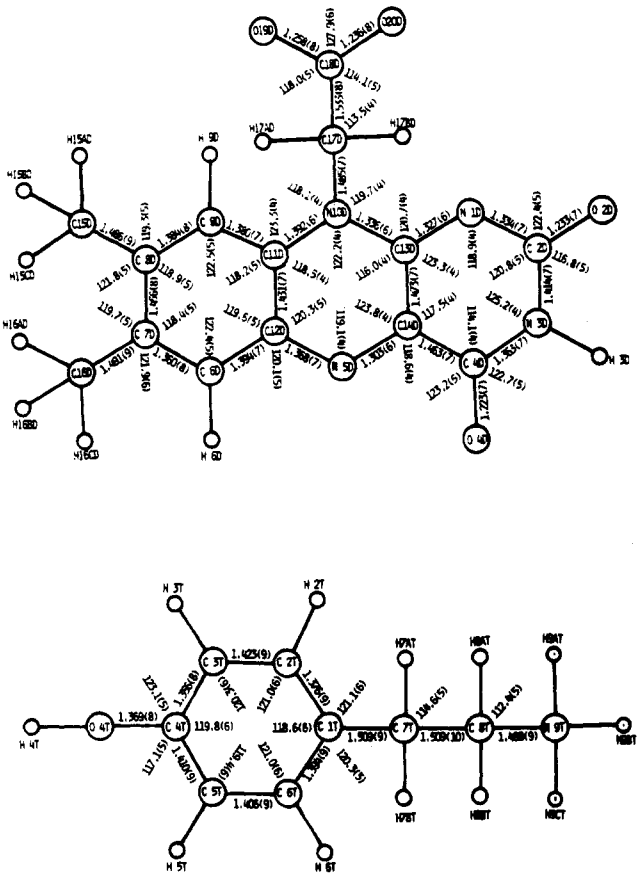

FIGURE 3: Complex II. Bond lengths (in angstroms) and angles (in degrees) between nonhydrogen atoms, along with the numbering used in this work.

maximum deviaion of 0.09 Å for C2D; the root mean square deviation of the 14 nonhydrogen atoms from the best plane is 0.027 Å. The dihedral angle between the least-squares planes of the benzenoid and pyrimidinoid portions of the isoalloxazine ring is 4.7°, so that the slight deformation observed for the pyrazinoid portion produced the boat conformation of the isoalloxazine ring. This conformation was also observed in the other oxidized flavin derivatives (Kuo et al., 1974; Scarbrough et al., 1977; Wells et al., 1974). The O2D and C16D atoms directly attached to the isoalloxazine ring deviate significantly from the plane (0.166 and 0.198 Å, respectively), probably due to the effects of hydrogen bonding and crystal packing. The bond lengths for the carboxyl group are almost identical and within their expected ranges as having no hydrogen atom. This group is almost planar and at approximately right angles to the isoalloxazine ring (dihedral angle = 80.5°).

The bond parameters of the TPA molecule agree well with the values found in the other TPA molecules: TPA (Inoue et al., 1978b), TPA picrate (Gartland et al., 1974), TPA phenylacetate (Inoue et al., 1978a), and TPA 1-thyminylacetate (Ishida et al., 1979c). The indole ring is planar with a maximum shift of 0.011 Å for C8T; the dihedral angle between the indole ring and the aminoethyl group is 80.5°. Selected torsion angles are listed in Table IV. The conformation of the TPA molecule is very similar to that of the most energetically stable TPA (Inoue et al., 1978b): the torsion angle of χ and ϕ are in the (+) anticlinal and (−) synclinal range, respectively.

Molecular Structure of Complex II. The covalent bonding parameters of the isoalloxazine ring are also in agreement with those of the oxidized "idealized" lumiflavin, although the agreement is not as good as in complex I. The average deviation from the idealized values is 0.014 Å. The only significant exception is that the distances of N1D–C2D (1.334 Å) and N10D–C13D (1.336 Å) are shorter than the idealized distances (1.368 and 1.362 Å, respectively). This tendency has also been observed in bis(riboflavin)·bis(cupric perchlorate) (Garland & Fritchie, 1974). The isoalloxazine ring is more planar than that of complex I; the root mean square deviation of the nonhydrogen atoms from the best plane is 0.007 Å, with a maximum deviation of 0.05 Å for C4D; the dihedral angle between the benzenoid and pyrimidinoid planes is 2.2°.

As is obvious from Table IV, the conformation of the DIA molecule is similar in both complexes. This conformation has been frequently observed in compounds having the carboxymethyl group attached to the heterocyclic nitrogen atom such as 9-adenylacetic acid [τ = 66.9°, ν = 7.7° (Voet, 1973); τ = 81.5°, ν = −3.9° (Ishida et al., 1979b)] and 1-thyminylacetic acid [τ = 66.9°, ν = 14.4° (Ishida et al., 1979c)]: these torsion angles are (+) synclinal for τ and synperiplanar for ν, respectively. The bond lengths and angles for the carboxyl group are also within the expected ranges as having no hydrogen atom. The carboxyl group is almost planar and at approximately right angles to the isoalloxazine ring (dihedral angle = 81.1°).

In the phenol ring of the TRA molecule, the mean C–C distance of 1.394 Å and the C4T–O4T distance of 1.369 Å are not significantly different from values found in tyramine hydrochloride (1.388 and 1.361 Å) (Tamura et al., 1974), *l*-tyrosine (1.390 and 1.369 Å) (Mostad et al., 1972), *l*-tyrosine hydrochloride (1.391 and 1.374 Å) (Frey et al., 1973), and *dl*-tyrosine (1.393 and 1.371 Å) (Mostad & Römming, 1973). The planarity of the benzene ring is reasonable compared with the other related compounds, and O4T and C7T atoms lie almost on the plane. The dihedral angle between the aminoethyl group and the benzene ring is 104.7°; the TRA molecule manifests a folded conformation, very similar to that of *l*-dopa (ω = 110.6°, θ = −63.3°) (Mostad et al., 1971).

Crystal Structure of Complex I. The stereoscopic packing diagram viewed down the *b* axis is shown in Figure 4. The layers formed by the stacking interactions of alternate DIA and TPA molecules are piled up in the *b* direction. These

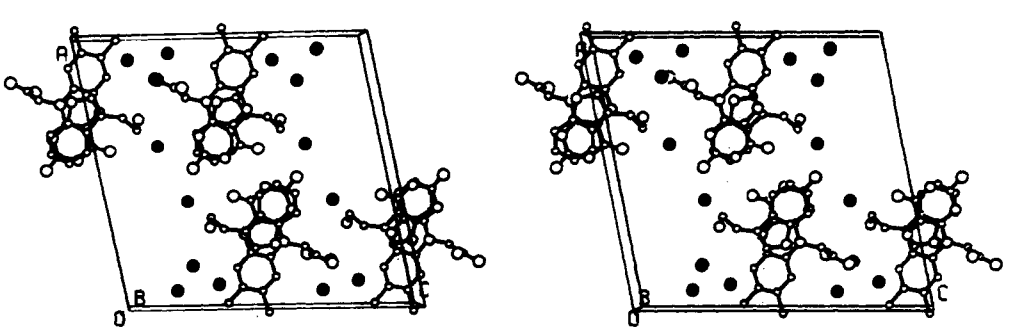

FIGURE 4: Stereoscopic packing diagrams of complex I viewed down the *b* axis. The full circles represent water molecules.

Table III: Atomic Coordinates for Nonhydrogen Atoms ($\times 10^4$) of Complexes I and II

complex I				complex II			
atom	x	y	z	atom	x	y	z
N1D[a]	3606 (2)	1918 (5)	6369 (2)	N1D	9128 (4)	2478 (4)	4163 (2)
C2D	4300 (2)	1444 (6)	6307 (2)	C2D	9459 (4)	3444 (5)	4501 (3)
O2D	4808 (1)	1474 (5)	6800 (1)	O2D	9713 (4)	4334 (3)	4209 (2)
N3D	4448 (1)	890 (5)	5652 (2)	N3D	9543 (4)	3484 (4)	5221 (2)
C4D	3952 (2)	745 (5)	5048 (2)	C4D	9309 (4)	2587 (4)	5632 (2)
O4D	4112 (1)	252 (4)	4494 (1)	O4D	9431 (4)	2657 (4)	6255 (2)
N5D	2682 (1)	1030 (4)	4580 (1)	N5D	8611 (4)	646 (4)	5610 (2)
C6D	1416 (2)	1195 (6)	4077 (2)	C6D	7908 (5)	−1302 (5)	5630 (3)
C7D	702 (2)	1524 (6)	4121 (2)	C7D	7548 (5)	−2309 (5)	5318 (3)
C8D	544 (2)	2211 (6)	4760 (2)	C8D	7521 (5)	−2382 (5)	4579 (3)
C9D	1092 (2)	2482 (6)	5331 (2)	C9D	7838 (5)	−1421 (5)	4223 (3)
N10D	2388 (2)	2252 (4)	5862 (2)	N10D	8529 (4)	571 (3)	4193 (2)
C11D	1823 (2)	2082 (5)	5288 (2)	C11D	8196 (4)	−399 (4)	4542 (2)
C12D	1982 (2)	1452 (5)	4649 (2)	C12D	8231 (4)	−339 (5)	5269 (2)
C13D	3086 (2)	1802 (2)	5808 (2)	C13D	8857 (4)	1556 (4)	4513 (2)
C14D	3198 (2)	1217 (5)	5128 (2)	C14D	8884 (4)	1544 (4)	5262 (2)
C15D	−242 (2)	2629 (7)	4826 (3)	C15D	7169 (6)	−3458 (5)	4200 (4)
C16D	103 (2)	1111 (8)	3505 (3)	C16D	7197 (6)	−3332 (5)	5709 (4)
C17D	2218 (2)	2786 (7)	6548 (2)	C17D	8590 (5)	472 (5)	3447 (2)
C18D	1869 (2)	1082 (6)	6885 (2)	C18D	7299 (6)	376 (5)	3029 (3)
O19D	1575 (2)	1545 (6)	7387 (2)	O19D	7324 (5)	−33 (4)	2452 (2)
O20D	1906 (2)	−537 (5)	6638 (2)	O20D	6357 (4)	720 (4)	3296 (2)
N1T	2350 (2)	7148 (5)	5456 (2)	C1T	6058 (5)	2310 (5)	6120 (3)
C2T	2214 (2)	6664 (6)	4758 (2)	C2T	5710 (5)	1396 (5)	5698 (3)
C3T	2841 (2)	6085 (6)	4547 (2)	C3T	5714 (5)	1486 (5)	4979 (3)
C4T	4158 (2)	5829 (6)	5293 (2)	C4T	6036 (5)	2488 (5)	4695 (3)
C5T	4552 (3)	6087 (7)	5954 (3)	O4T	6046 (4)	2633 (4)	4007 (2)
C6T	4208 (3)	6745 (7)	6498 (2)	C5T	6380 (6)	3442 (5)	5116 (3)
C7T	3479 (3)	7153 (6)	6380 (2)	C6T	6384 (6)	3340 (5)	5827 (3)
C8T	3081 (2)	6886 (6)	5713 (2)	C7T	6061 (6)	2217	6883 (3)
C9T	3409 (2)	6208 (5)	5160 (2)	C8T	7345 (6)	2066 (6)	7275 (3)
C10T	2924 (2)	5442 (6)	3833 (2)	N9T	7984 (5)	1006 (4)	7074 (2)
C11T	3367 (2)	6813 (7)	3461 (2)	O1W	9618 (5)	9029 (6)	2122 (2)
N12T	3015 (2)	8715 (5)	3341 (2)	O2W	4861 (7)	9676 (6)	1767 (4)
O1W	594 (2)	782 (6)	1815 (2)	O3W	3700 (7)	818 (6)	2808 (5)
O2W	885 (2)	5821 (6)	3268 (2)	O4W	1024 (10)	1674 (9)	2538 (4)
O3W	1616 (2)	8301 (5)	2497 (2)				
O4W	3952 (2)	1266 (6)	2836 (2)				

[a] The suffixes D, T, and W in the atom designations refer to DIA, TPA (complex I) or TRA (complex II), and water molecules, respectively.

Table IV: Selected Torsion Angles (deg) of DIA, TPA, and TRA Molecules

bond sequence	complex I	complex II
C13D–N10D–C17D–C18D	−100.8	−111.5
C11D–N10D–C17D–C18D (τ)	74.0	72.1
N10D–C17D–C18D–O19D	−165.6	−160.1
N10D–C17D–C18D–O20D (ν)	14.3	20.6
C2T–C3T–C10T–C11T (χ)	111.9	
C9T–C3T–C10T–C11T	−68.6	
C3T–C10T–C11T–N12T (ϕ)	−62.0	
C2T–C1T–C7T–C8T (ω)		102.8
C1T–C7T–C8T–N9T (θ)		−60.3

layers are stabilized by van der Waals contacts with the neighboring layers and by hydrogen bondings with four water molecules existing among the layers. The network of the hydrogen bonds is shown in Figure 5; their distances are also indicated. All of the hydrogen bonds which DIA and TPA molecules are capable of forming are formed; they fall within the normally observed ranges for such interactions (Ondik & Smith, 1968). The O4D and N5D atoms of DIA, which are the chelate sites of the metal ion (Langhoff & Fritchie, 1970), are occupied by two hydrogen bonds of N12T---O4D and N12T---N5D. These and N1T---O20D hydrogen bonds form an intermolecular complex of DIA and TPA molecules (Figures 5 and 6). The DIA molecule forms a dimer with two hydrogen bonds around a center of symmetry (N3D---O4D). The four water molecules are linked to the neighboring DIA,

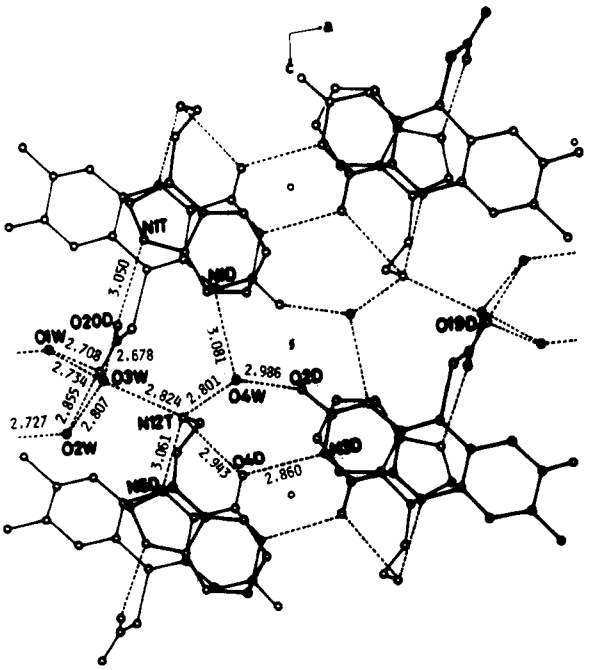

FIGURE 5: Possible hydrogen-bonding scheme (dotted lines) in complex I, viewed down the b axis.

TPA, and water molecules by three to four hydrogen bonds within reasonable distances; they stabilize the molecular

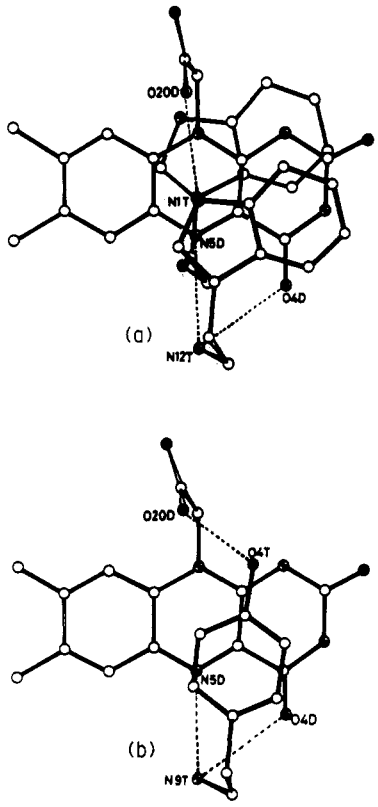

FIGURE 6: Stacking mode of nearest-neighboring donor–acceptor pairs, projected on the isoalloxazine ring. The hydrogen bonds are shown by dotted lines. (a) Complex I; (b) complex II.

packing of the DIA and TPA molecules.

Crystal Structure of Complex II. Figure 7 shows a stereodiagram illustrating the packing of complex II viewed down the *a* axis. The network of the hydrogen bondings observed in the crystal structure is shown in Figure 8. The layers constituting ...-DIA-TRA-TRA-DIA-DIA-... molecular arrangements are arranged parallel to the *a* axis. Similar to complex I, they are stabilized by normal van der Waals contacts with neighboring layers and by hydrogen bondings with water molecules. The hydrogen bonding modes are also very similar to those of complex I. The hydroxyl group of the TRA molecule is hydrogen bonded to O20D of the DIA molecule; N9T is bonded to the O4D and N5D atoms (chelate site) of DIA. These hydrogen bonds form an intermolecular complex of DIA and TRA molecules (Figures 6 and 8). DIA molecules related by one center of symmetry ($2 - x$, $1 - y$, $1 - z$) are linked by two hdyrogen bonds (N3D---O2D) and form a dimer almost parallel to the *b*–*c* plane. On the other hand, the DIA molecules related by another center of symmetry ($2 - x$, $-y$, $1 - z$) are associated with each other by the normal stacking interactions. The two isoalloxazine rings overlap extensively. There are four interatomic distances less than normal van der Waals separation, 3.4 Å: N3D–C8D, 3.381 Å; C4D–C9D, 3.330 Å; N5D–N10D, 3.360 Å; C11D–C14D, 3.384 Å. The average distance between the least-squares planes of these centrosymmetrically related, and therefore parallel, isoalloxazine rings is 3.393 Å. This extensive overlapping has also been observed in bi(lumiflavin-2,6-diamino-9-ethylpurine) (Scarbrough et al., 1977) and 10-[3-(3-carbamoyl-1-pyridinyl)propyl]-7,8-dimethylisoalloxazine (Porter & Voet, 1978). Four water molecules, present among the layers consisting of DIA and TRA molecules, participate in two to four hydrogen bondings within reasonable distances and angles, thereby stabilizing the molecular packing of DIA and TRA molecules.

Stacking Modes between Isoalloxazine and Indole Rings and between Isoalloxazine and Phenol Rings. Figure 6 illustrates the stacking modes of the isoalloxazine–indole and isoalloxazine–phenol rings observed in crystal structures. The planes of the indole and phenol rings are almost parallel to the plane of the isoalloxazine ring; the dihedral angle is 3.0° for both paris of complex I and is 0.1° for one pair of complex II. Many short contacts < 3.4 Å are observed in the upper pair in part a and in part b of Figure 6, which are ranging in 3.221–3.392 Å for complex I and in 3.256–3.381 Å for complex II. The average interplanar spacing in the area of overlap is 3.179 Å in the former and 3.180 Å in the latter case. In these pairs, the observed parallel stacking and interplanar spacing which were significantly less than the normal van der Waals separation suggest strongly that both complexes are associated by what is clearly a π_D–π_A charge transfer from their donor rings to the lowest unoccupied orbital of the isoalloxazine ring in the ground state.

Furthermore, common characteristics found in these stacking pairs are as follows. (1) The indole and phenol rings lie above the pyrimidinoid and pyrazinoid portions, not above the benzenoid portion, of the isoalloxazine ring. Similar overlapping has been observed in the crystal structures of the 10-propylisoalloxazine·bis(naphthalene-2,3-diol) (Kuo et al.,

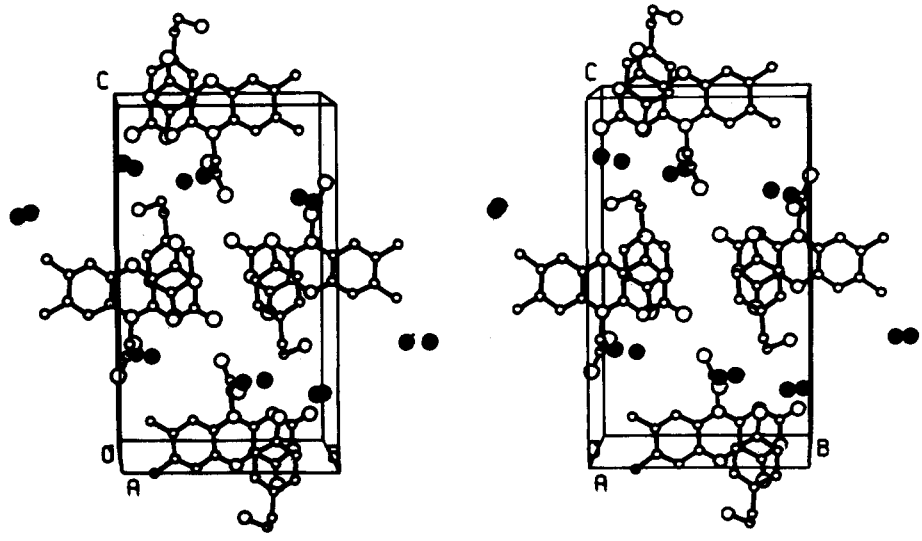

FIGURE 7: Stereoscopic packing diagrams of complex II viewed down the *a* axis. The full circles represent water molecules.

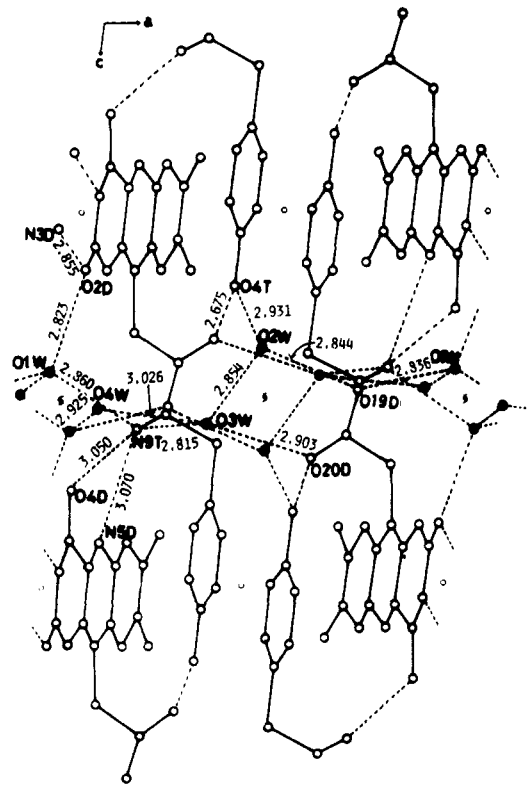

FIGURE 8: Possible hydrogen-bonding scheme (dotted lines) in complex II, viewed down the *b* axis.

1972), the 5′-bromo-5′-deoxyadenosine·riboflavin (Voet & Rich, 1971), and the adenine·riboflavin (Fujii et al., 1977), and similar interactions have been suggested to exist in the native old yellow enzyme–phenol interaction (Nishina et al., 1980) and in flavin–tryptophan and/or –tyrosine interactions of egg white flavoprotein (Nishikimi & Kyogoku, 1973). These observations lead us to posit that both the indole and phenol rings interact strongly with the pyrimidinoid and pyrazinoid portions of the isoalloxazine ring of flavin coenzymes. (2) The donor atoms of TPA and TRA molecules interact strongly with the N1D and N5D atoms (reduction site) of the DIA molecule: N1D–C7T, N5D–C2T, and N5D–N1T in complex I; N1D–O4T, N5D–C2T, and N5D–C3T in complex II. These short contacts could play an important role in raising the proton-accepting ability of the N1D and N5D atoms by electron transfer from the donor atoms, thereby facilitating the transition of oxidized flavin to the semiquinone state. (3) Both the indole and phenol rings are strongly stacked from the upper, not from the lower, site of the isoalloxazine ring having a specified orientation as shown in Figure 6. The similar characteristics of both stacked pairs suggest that the tryptophan and tyrosine residues have the same function in the binding with the flavin coenzyme and in the oxidation–reduction reaction in flavoprotein.

Orientations between Isoalloxazine and Indole Rings and between Isoalloxazine and Phenol Rings. Figure 9 shows the orientations of the indole and phenol rings to the fixed isoalloxazine ring. The calculated permanent dipole moments (debye) and their vectors for the ring planes of DIA, TPA, and TRA molecules obtained by using the CNDO/2 method and the free valences of their atoms (Pullman & Pullman, 1963) are also indicated.

Although the possibility cannot be ruled out that the dipole–(induced) dipole interaction is largely responsible for specifying the mutual orientation of the two associated molecules, e.g., base stacking of nucleic acid (Bugg et al., 1971), this interaction need not be strong in these charge-transfer complexes. The dipole moments of both stacked pairs are almost completely uncoupled, suggesting that the crystal packing forces have overcome the effects of dipole–dipole coupling. The distribution of their atomic free valences indicates that the mutual orientation of both rings depends mainly on the interaction of atoms with large free valences: N1D–C7T, N5D–C2T, and N5D–N1T for complex I; N1D–O4T, N5D–C2T, and N5D–C3T for II, which are also the pairs exhibiting short contacts.

Interactions between DIA and TPA Molecules and between DIA and TRA Molecules in Solution. Figure 10 shows the absorption difference spectra of complexes I and II against DIA plus TPA and against DIA plus TRA molecules, respectively. Remarkable charge-transfer bands are noted in the 450–620-nm (λ_{max} = 512 nm) range for complex I and the 470–560-nm (λ_{max} = 520 nm) range for complex II. Similar charge-transfer bands are also observed in the equimolar FMN–Trp, FAD–Trp, and FMN–Tyr mixtures. The Job plot (Job, 1925) clearly indicates that both complexes I and II have 1:1 stoichiometry in solution as well as in the crystalline state. The association constants of both complexes were evaluated by the Benesi–Hildebrand equation (Benesi & Hildebrand, 1949) by using the λ_{max} of their charge-transfer bands under conditions in which [TPA] and [TRA] $\gg$ [DIA]. The obtained constant (K_c) is 51 (5) M^{-1} for complex I and is 47 (5) M^{-1} for complex II. These values are very similar

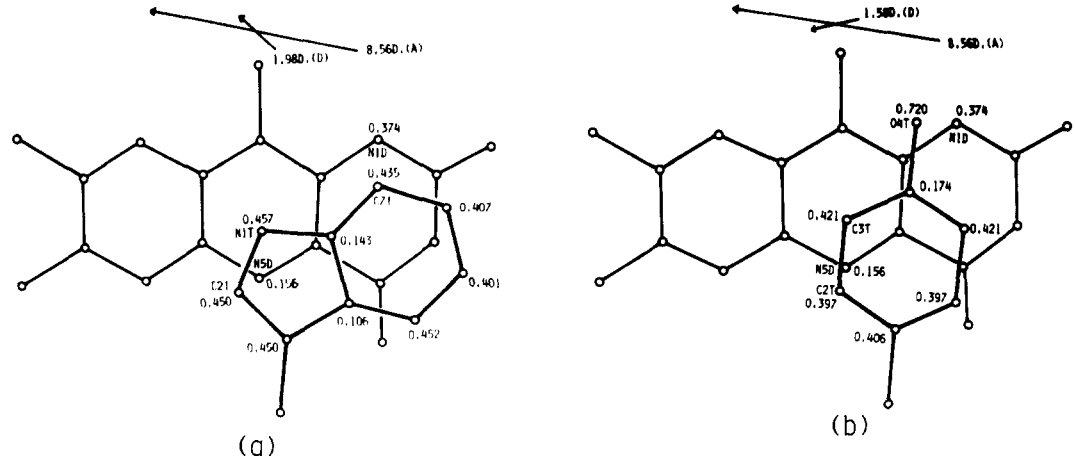

FIGURE 9: Values of free valences on atoms of donor–acceptor pairs found in the ground state of structures of complexes I (a) and II (b), viewed perpendicular to the isoalloxazine ring. The relative magnitudes (debye) and directions of the calculated permanent dipole moments for the ground states of the donor (D) and acceptor (A) are shown above the respective structures.

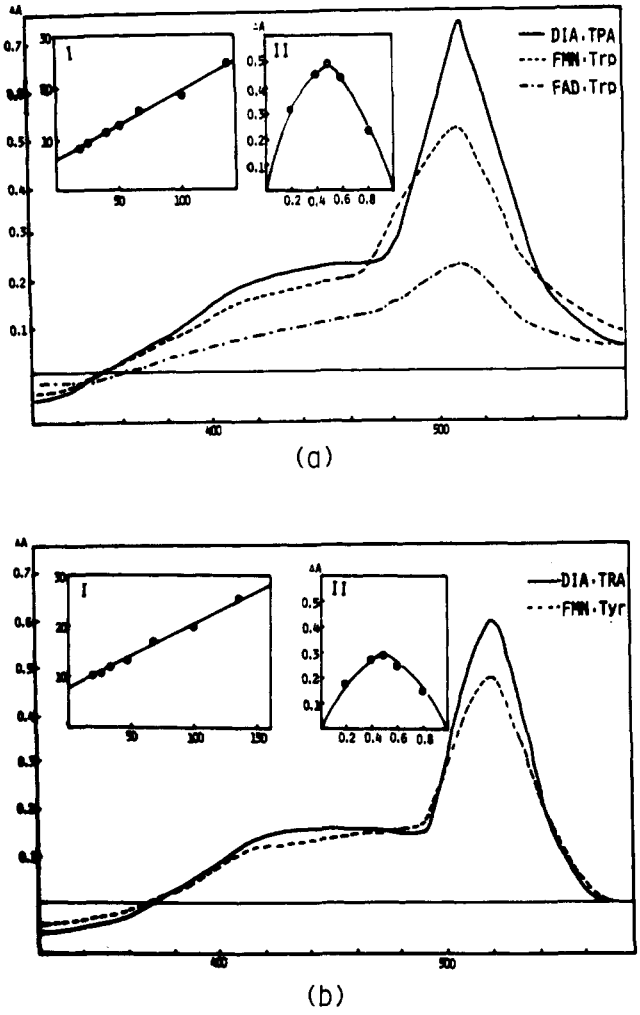

FIGURE 10: Charge-transfer difference spectra for 1:1 mixtures of DIA–TPA, FMN–Trp, and FAD–Trp (a) and of DIA–TRA and FMN–Tyr (b). All concentrations were 0.6×10^{-2} M in 0.025 M phosphate buffer containing 30% ethanol (pH 6.9). (Insert I) Benesi–Hildebrand plot for the DIA–TPA or DIA–TRA mixture with the donor molecule as the variable. Absorbance was measured at 512 nm (for DIA–TPA) or 520 nm (for DIA–TRA) at 25 °C. The concentration of DIA was kept at 4.8×10^{-4} M, and that of TPA or TRA was varied from 0.5×10^{-2} to 5.0×10^{-2} M. (Insert II) Job plot for the DIA–TPA or DIA–TRA mixture with the summation of [TPA] or [TRA] plus [DIA] as the constant (0.5×10^{-2} M). Absorbance was measured at 512 nm for DIA–TPA or 520 nm for DIA–TRA at 25 °C.

to those of the FMN–Trp complex (K_c = 56–98 M^{-1}) (Draper & Ingraham, 1970; Isenberg & Szent-Györgyi, 1958; Pereira & Tollin, 1967; Wilson, 1966), the riboflavin–Trp complex (K_c = 42 (3) M^{-1}), the FMN–Tyr complex (K_c = 66 (12) M^{-1}), and the riboflavin–Tyr complex (K_c = 73 (12) M^{-1}) (Draper & Ingraham, 1970). Therefore, complexes I and II may be considered as the most suitable models for studies on the flavin–tryptophan and flavin–tyrosine interactions in flavoprotein, respectively.

To elucidate the stacking modes of the these complexes in solution,we measured the PMR spectra of TPA and TRA alone and in a mixture with DIA (Figure 11). Peak assignments were according to Föry et al. (1970), Hiremath & Hosmane (1973), and Kolodny et al. (1977). The spectral changes produced by the addition of DIA are very similar. The chemical shifts of the aromatic protons of TPA and TRA molecules are upfield upon mixing with the DIA molecule (~0.1-ppm upfield shifts, on average, at a molar ratio of 5:2 for TPA–DIA and TRA–DIA), while the protons of the side chains reversibly shift downfield by ~0.1 ppm. On the other

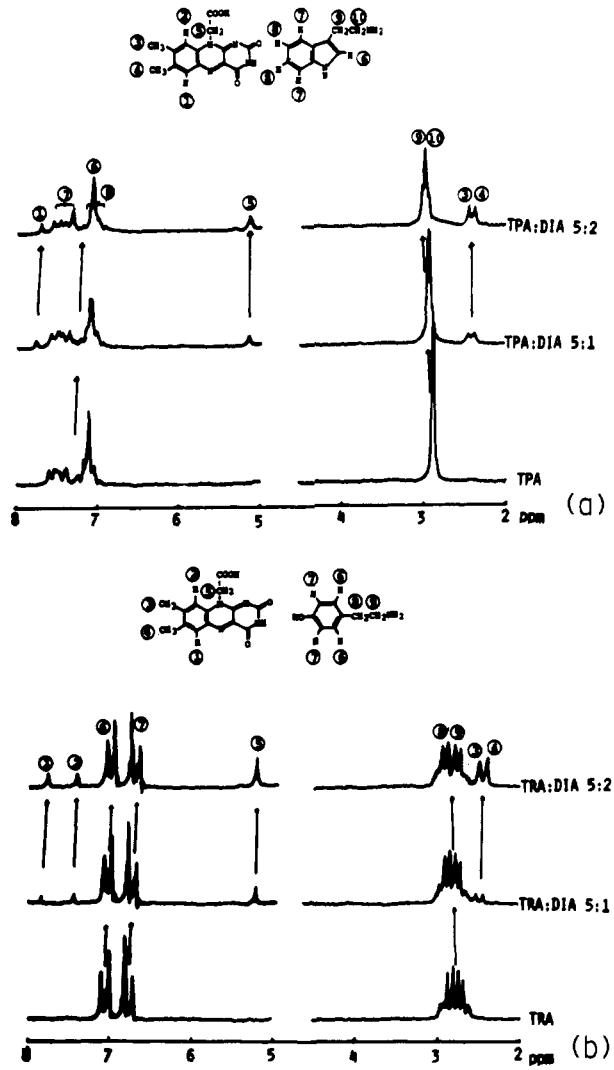

FIGURE 11: PMR spectra of TPA, TPA/DIA = 5:1, and TPA/DIA = 5:2 mixtures (a) and of TRA, TRA/DIA = 5:1, and TRA/DIA = 5:2 mixtures (b), dissolved in 50% CD_3OD–D_2O solution. The initial concentration of TPA or TRA was 2.0×10^{-2} M; DIA was added to the solution. Chemical shifts were adjusted by reference to DSS as an internal standard. We could not measure PMR spectra of mixtures having a molar ratio of DIA to donor molecule larger than 2:5 because of the appearance of precipitates.

hand, upfield shifts of the benzenoid protons of DIA were observed upon increasing the DIA concentration, while the dimethyl and side-chain protons remained almost unchanged. The changes in the chemical shifts may be explicable by ring-current effects due to the stacking interactions. The observed shifts of respective protons suggest that both the indole and phenol rings may stack directly over the whole of the isoalloxazine ring, while the side chains are far from it. Such stacking modes are rather different from those observed in crystal structures, in which both rings are located on the pyrimidinoid and pyrazinoid portions of the isoalloxazine ring.

In conclusion, our present study provided the following information: (1) The existence of strong charge-transfer interactions between indole and isoalloxazine rings and between phenol and isoalloxazine rings, in their ground states, were shown by X-ray analyses of complexes I and II. These charge-transfer forces may represent important factors in the tight binding of flavin coenzymes to apoproteins in flavoproteins. (2) The binding sites of both the indole and phenol rings to the isoalloxazine ring are in the pyrimidinoid and pyrazinoid portions. (3) Because of the short contacts between the reducible atoms of the isoalloxazine and the donor atoms,

the reduction potential of the oxidized isoalloxazine ring to the semiquinone state is reduced by the charge transfer from these donor atoms; consequently, tryptophan and tyrosine residues may facilitate the reduction of the oxidized flavins in flavoproteins. (4) The similar stacking modes observed in the stacked pairs of complexes I and II suggest that both the tryptophan and tyrosine residues existing at the binding site of flavins may have the same biological functions in the effective oxidation–reduction catalyses of flavoproteins.

Supplementary Material Available

Observed and calculated structure factors, thermal parameters, coordinates of hydrogen atoms, equations of the least-squares planes and deviations of atoms from these planes (Å), distances (Å) of hydrogen bonds and short contacts < 3.5 Å, and figures of stacking between DIA molecules in complex II, projected on the isoalloxazine ring, and between indole and isoalloxazine rings (complex I) and phenol and isoalloxazine rings (complex II), projected parallel to the isoalloxazine ring, along with distances < 3.4 Å (48 pages). Ordering information is given on any current masthead page.

References

Andrews, L. J., MacKnight, M. L., Ryan, J., & Tollin, G. (1973) *Biochem. Biophys. Res. Commun. 55*, 1165.

Ashida, T. (1973) in *The Universal Crystallographic Computing System* (Ashida, T., Ed.) pp 20, 21, 27, 55–65, The Computation Center, Osaka University, Osaka, Japan.

Benesi, H. A., & Hildebrand, J. H. (1949) *J. Am. Chem. Soc. 71*, 2703.

Blankenhorn, G. (1978) *Eur. J. Biochem. 82*, 155.

Bugg, C. E., Thomas, J. M., Sundaralingam, M., & Rao, S. T. (1971) *Biopolymers 10*, 175.

Burnett, R. M., Darling, G. D., Kendall, D. S., LeQuesne, M. E., Mayhew, S. G., Smith, W. W., & Ludwig, M. L. (1974) *J. Biol. Chem. 249*, 4383.

Cromer, D. T., & Waber, J. T. (1974) *Int. Tables X-Ray Crystallogr. 4*, 71–73.

Draper, R. D., & Ingraham, L. L. (1970) *Arch. Biochem. Biophys. 139*, 265.

Fall, H. H., & Petering, H. G. (1956) *J. Am. Chem. Soc. 78*, 377.

Föry, W., MacKenzie, R. E., & McCormick, D. B. (1968) *J. Heterocycl. Chem. 5*, 625.

Föry, W., MacKenzie, R. E., Wu, F. Y. H., & McCormick, D. B. (1970) *Biochemistry 9*, 515.

Frey, M. N., Koetzle, T. F., Lehmann, M. S., & Hamilton, W. C. (1973) *J. Chem. Phys. 58*, 2547.

Fujii, S., Kawasaki, K., Sato, A., Fujiwara, T., & Tomita, K. (1977) *Arch. Biochem. Biophys. 181*, 363.

Garland, W. T., Jr., & Fritchie, C. J., Jr. (1974) *J. Biol. Chem. 249*, 2228.

Gartland, G. L., Freeman, G. R., & Bugg, C. E. (1974) *Acta Crystallogr., Sect. B 30*, 1841.

Germain, G., Main, P., & Woolfson, M. M. (1971) *Acta Crystallogr., Sect. A 27*, 368.

Hiremath, S. P., & Hosmane, R. S. (1973) *Adv. Heterocycl. Chem. 15*, 277.

Inoue, M., Sakaki, T., Fujiwara, T., & Tomita, K. (1978a) *Bull. Chem. Soc. Jpn. 51*, 1123.

Inoue, M., Sakaki, T., Wakahara, A., & Tomita, K. (1978b) *Biochim. Biophys. Acta 543*, 123.

Inoue, M., Shibata, M., & Ishida, T. (1980) *Biochem. Biophys. Res. Commun. 93*, 415.

Isenberg, I., & Szent-Györgyi, A. (1958) *Proc. Natl. Acad. Sci. U.S.A. 44*, 857.

Ishida, T., Inoue, M., Fujiwara, T., & Tomita, K. (1979a) *J. Chem. Soc., Chem. Commun.*, 358.

Ishida, T., Inoue, M., Senda, S., & Tomita, K. (1979b) *Bull. Chem. Soc. Jpn. 52*, 2953.

Ishida, T., Inoue, M., & Tomita, K. (1979c) *Acta Crystallogr., Sect. B 35*, 1642.

Ishida, T., Mitoguchi, S., Miyamoto, Y., Tomita, K., & Inoue, M. (1980) *Biochim. Biophys. Acta 609*, 158.

Job, P. (1925) *C. R. Hebd. Seances Acad. Sci. 180*, 928.

Kenney, W. C., Edmondson, D. E., & Singer, T. P. (1974) *Eur. J. Biochem. 48*, 449.

Kolodny, N. H., Neville, A. C., Coleman, D. L., & Zamecnik, P. C. (1977) *Biopolymers 16*, 259.

Kuo, M. C., Dunn, J. B. R., & Fritchie, C. J., Jr. (1972) *J. Chem. Soc., Chem. Commun.*, 205.

Kuo, M. C., Dunn, J. B. R., & Fritchie, C. J., Jr. (1974) *Acta Crystallogr., Sect. B 30*, 1766.

Langhoff, C. A., & Fritchie, C. J., Jr. (1970) *J. Chem. Soc., Chem. Commun.*, 20.

Mayhew, S. G., & Ludwig, M. L. (1975) *Enzymes, 3rd Ed. 12*, 57–118.

McCormick, D. B. (1970) *Experientia 26*, 243.

McCormick, D. B. (1977) *Photochem. Photobiol. 26*, 169.

Mostad, A., & Römming, C. (1973) *Acta Chem. Scand. 27*, 401.

Mostad, A., Ottersen, T., & Römming, C. (1971) *Acta Chem. Scand. 25*, 3549.

Mostad, A., Nissen, H. M., & Römming, C. (1972) *Acta Chem. Scand. 26*, 3819.

Nishikimi, M., & Kyogoku, Y. (1973) *J. Biochem. (Tokyo) 73*, 1233.

Nishina, Y., Kitagawa, T., Shiga, K., Watari, H., & Yamano, T. (1980) *J. Biochem. (Tokyo) 87*, 831.

Nygaard, A. P., & Theorell, H. (1955) *Acta Chem. Scand. 9*, 1587.

Ondik, H., & Smith, D. (1968) *Int. Tables X-Ray Crystallogr. 3*, 273.

Pereira, J. F., & Tollin, G. (1967) *Biochim. Biophys. Acta 143*, 79.

Pople, J. A., & Segal, G. A. (1966) *J. Chem. Phys. 44*, 3289.

Porter, D. J. T., & Voet, D. (1978) *Acta Crystallogr., Sect. B 34*, 598.

Pullman, B., & Pullman, A. (1963) in *Quantum Biochemistry*, Interscience, New York.

Ryan, J., & Tollin, G. (1973) *Biochemistry 12*, 4550.

Scarbrough, F. E., Shieh, H. S., & Voet, D. (1977) *Acta Crystallogr., Sect. B 33*, 2512.

Slifkin, M. A. (1971) in *Charge Transfer Interactions of Biomolecules*, pp 132–171, Academic Press, New York.

Steczko, J., & Ostrowski, W. (1975) *Biochim. Biophys. Acta 393*, 253.

Strittmatter, P. (1961) *J. Biol. Chem. 236*, 2329.

Tamura, K., Wakahara, A., Fujiwara, T., & Tomita, K. (1974) *Bull. Chem. Soc. Jpn. 47*, 2682.

Tu, S. C., & McCormick, D. B. (1973) *J. Biol. Chem. 248*, 6339.

Voet, D. (1973) *J. Am. Chem. Soc. 95*, 3763.

Voet, D., & Rich, A. (1971) *Proc. Natl. Acad. Sci. U.S.A. 68*, 1151.

Wang, M., & Fritchie, C. J., Jr. (1973) *Acta Crystallogr., Sect. B 29*, 2040.

Watenpaugh, K. D., Sieker, L. C., & Jensen, L. H. (1973) *Proc. Natl. Acad. Sci. U.S.A. 70*, 3857.

Wells, J. L., Trus, B. L., Johnston, R. M., Marsh, R. E., & Fritchie, C. J., Jr. (1974) *Acta Crystallogr., Sect. B 30*, 1127.
Wilson, J. E. (1966) *Biochemistry 5*, 1351.
Wu, F. Y. H., & McCormick, D. B. (1971) *Biochim. Biophys. Acta 236*, 479.
Wu, F. Y. H., Tu, S. C., Wu, C. W., & McCormick, D. B. (1970) *Biochem. Biophys. Res. Commun. 41*, 381.

Reactive Lysyl of Myosin Subfragment 1: Location on the 27K Fragment and Labeling Properties†

Tetsu Hozumi*,‡ and Andras Muhlrad§

ABSTRACT: The limited tryptic digestion of the heavy chain of chymotryptic myosin subfragment 1 resulted in five peptides with approximate molecular weights of 75K, 50K, 29.5K, 27K, and 20K. Of the five peptides, two, 75K and 29.5K, were transient and disappeared during the digestion. Our data suggest that the 27K fragment is generated by two parallel routes: directly from the 75K fragment and through a 29.5K precursor. A method was developed to isolate the final products, 50K, 27K, and 20K fragments, of the tryptic hydrolysis of the heavy chain of myosin subfragment 1. Using this method, it was found that the reactive lysyl residue, labeled by a trinitrophenyl moiety, resides in the 27K fragment. The reactive lysyl residue was also present in the 29.5K fragment. The trinitrophenylation of the reactive lysyl residue was inhibited by magnesium pyrophosphate in the 27K but not in the 29.5K fragment. This may indicate that the two routes of generating the 27K peptide correspond to the proteolysis of two qualitatively different subfragment-1 heads as suggested by Tonomura [Tonomura, Y. (1972) *Muscle Proteins, Muscle Contraction and Cation Transport*, University of Tokyo Press, Tokyo, and University Park Press, Baltimore].

It is generally believed that myosin subfragment 1 (S-1)[1] is the segment of the myosin molecule that catalyzes the hydrolysis of adenosine 5′-triphosphate (ATP) and thereby impels actin. So the structure and "internal mechanics" of S-1 acquire great importance. Groups with various suggestive functionalities (reactive thiols, a reactive lysine, certain tryptophans, etc.) reside on S-1. Balint et al. (1978) showed that limited tryptic hydrolysis cuts S-1 into three major fragments (so-called "50", "27K", and "20K") without much additional proteolysis. Recently, Mornet et al. (1979) and Yamamoto & Sekine (1979) showed that the 50K/20K cut abolishes actin activation while leaving unaffected the various adenosine triphosphatases (ATPases) of S-1 alone. Szilagyi et al. (1979) showed that at least the purine moiety of the ATP substance binds to the 27K fragment. However, groups that strongly affect ATPase, such as the reactive thiols "SH_1" and "SH_2", reside on the 20K fragment (Balint et al., 1978). Kassab has suggested to us that perhaps the P–O–P–O–P moiety of ATP binds to the 20K fragment. The researches of Balint et al. (1978) and of Mornet et al. (1979) opened a new line of investigation. Locating known functionalities among the fragments is an early step along this line. Here, we show that the reactive lysyl residue (RLR) resides on the 27K fragment.[2] We also report observations indicating that among the final products the 27K RLR-bearing fragments are generated by two routes of proteolysis. This would be expected if the starting substrate (S-1) were of two qualitatively different kinds.

The RLR is defined by its reaction with 2,4,6-trinitrobenzenesulfonate (TNBS), and by the consequent effects on myosin ATPase (Kubo et al., 1960; Fabian & Muhlrad, 1968). Under the conditions employed here, binding and enzyme kinetic studies (Muhlrad & Takashi, 1980) indicate that about 70% of the trinitrophenyl (TNP) group that binds to S-1 binds to the RLR; presumably 30% binds to the remaining 82 lysyls of S-1 and has no enzymatic effects.

Materials and Methods

Chemicals. TNBS and *N*-[[(iodoacetyl)amino]ethyl]-5-naphthylaminesulfonic acid (IAEDANS) were from Aldrich Chemical Co. [^{3}H]TNBS, an Amersham product, was a generous gift from Professor Y. Tonomura. TPCK-trypsin, soybean trypsin inhibitor, and chymotrypsin were from Worthington Biochemical Co. All other chemicals were of reagent grade.

Proteins. Myosin and actin from back and leg muscles of rabbits were prepared by well-established methods [Tonomura et al. (1966) and Spudich & Watt (1971), respectively]. S-1 was prepared by digestion of myosin filaments with chymotrypsin (Weeds & Taylor, 1975) and purified by filtration through Sephacryl S-200 in 20 mM *N*-tris(hydroxymethyl)-methyl-2-aminoethanesulfonic acid (Tes), pH 7.0.

Protein Concentrations. Unlabeled myosin and S-1 concentrations were calculated from their absorbances, assuming

† From the Cardiovascular Research Institute, University of California, San Francisco, San Francisco, California 94143. *Received September 5, 1980; revised manuscript received January 6, 1981.* This research was supported by Grants HL-166683 (U.S. Public Health Service Program Project), PCM-75-22698 (National Science Foundation), and 60-008 (American Heart Association).

‡ Career Investigator Fellow of the American Heart Association. Present address: Department of Physiology, Nagoya City University Medical School, Nagoya, 467, Japan.
§ Senior Investigator of the Muscular Dystrophy Association. Present address: Department of Oral Biology, Hebrew University—Hadassah School of Dental Medicine, Jerusalem, Israel.

[1] Abbreviations used: S-1, myosin subfragment 1; RLR, reactive lysyl residue; TNBS, 2,4,6-trinitrobenzenesulfonate; TNP, trinitrophenyl; IAEDANS, *N*-[[(iodoacetyl)amino]ethyl]-5-naphthylaminesulfonic acid; TPCK-trypsin, L-1-(tosylamido)-2-phenylethyl chloromethyl ketone treated trypsin; Tes, *N*-tris(hydroxymethyl)methyl-2-aminoethanesulfonic acid; PP_i, inorganic pyrophosphate; $NaDodSO_4$, sodium dodecyl sulfate.

[2] Although we are unacquainted with the approach or details of their as yet unpublished work, we are aware that Tonomura and his associates reached this same conclusion well before us.

0006-2960/81/0420-2945$01.25/0